SIMS Proceedings Papers

SURFACE and INTERFACE ANALYSIS

Received: 11 September 2009 Revised: 22 March 2010 Accepted: 22 March 2010 Published online in Wiley Online Library: 1 June 2010

(wileyonlinelibrary.com) DOI 10.1002/sia.3509

Retrospective sputter depth profiling using 3D mass spectral imaging

Leiliang Zheng,[a] Andreas Wucher[b]* and Nicholas Winograd[a]

A molecular multilayer stack composed of alternating Langmuir-Blodgett films was analyzed by ToF-SIMS imaging in combination with intermediate sputter erosion using a focused C_{60}^+ cluster ion beam. From the resulting dataset, depth profiles of any desired lateral portion of the analyzed field-of-view can be extracted in retrospect, allowing the influence of the gating area on the apparent depth resolution to be assessed. In a similar way, the observed degradation of depth resolution with increasing depth of the analyzed interface can be analyzed in order to determine the 'intrinsic' depth resolution of the method.

Keywords: molecular depth profiling; 3D analysis; depth resolution; organic multilayer analysis

Introduction

Molecular sputter depth profiling using cluster ion projectiles has attracted significant interest over the past few years.[1–6] On the road to quantitative three-dimensional chemical characterization of surfaces and thin film systems at the molecular level, it is essential to understand the fundamental concepts behind molecular depth profiling and evaluate the physical concepts limiting the depth resolution attainable in this type of analysis. Using Langmuir-Blodgett multilayer systems,[7] we have investigated the dependence of measured interface widths on various instrumental parameters including beam energy, impact angle, sample temperature and interface depth.[8] It was found that the apparent depth resolution degrades as a function of eroded depth. This observation can be caused by a number of different mechanisms, some of which relate to instrumental and sample artifacts, while others represent fundamental issues regarding the sputter depth profiling method itself. It is the purpose of the present paper to demonstrate how three-dimensional imaging can be used in order to identify, distinguish and – at least partly – eliminate these effects from a measured dataset, thus allowing the intrinsic (static) limit of the achievable depth resolution to be determined.

Experimental

The langmuir-blodgett (LB) film preparation and characterization have been described in detail elsewhere.[7] Six alternating multilayer films of barium-arachidate (AA) and barium dimyristoyl phosphatidate (DMPA) of about 50 nm thickness (~20 LB layers) were deposited on a silicon substrate. Three-dimensional imaging was performed using a TOF-SIMS instrument[9] equipped with a 40-keV C_{60}^+ ion source aiming at the target surface at an angle of 40° relative to the surface normal. Depth profiling was performed by alternating between sputter erosion and data acquisition cycles. During data acquisition, static SIMS images were collected accumulating 20 shots/pixel with 128 × 128 pixels covering a ~400 μm^2 raster area. All detected secondary ions were registered, and the three-dimensional distribution of any desired mass can be extracted in retrospect from the acquired dataset. Sputter erosion was performed with the ion beam switched to direct current (d.c.) mode and digitally rastered over the same pixels as during image acquisition. In order to minimize material redeposition effects as known from FIB technology, a sputter erosion cycle of predefined time was divided into a number of fast raster scans in order to limit the dwell time on each pixel to about 10 µs per scan. Even though the spot size of ~10 µm was larger than the pixel size (3 µm), a dithering technique was used to ensure a homogenous sputter erosion in spite of the digital raster scan.

Retrospective depth profiles were constructed from the acquired image stack by integrating the measured signal $S(i, j, k)$ over the desired mass range within a range of pixels (j, k) in each image (i). As described elsewhere, the accumulated ion fluence was converted into eroded depth by interpolating between the erosion rates of AA and DMPA based on the integrated signals $S(i)$. Throughout the analysis, representative molecular signals of AA and DMPA at m/z 463 and m/z 525 were used along with a substrate signal at m/z 112 for Si_4^+.

Results and Discussion

Sputter depth profile analysis is often influenced by a laterally inhomogenous erosion rate leading to the development of macroscopic surface topography at the bottom of the eroded sputter crater. In addition, it is well known that ion bombardment can produce microscopic surface topography (roughening) which may accumulate with increasing ion fluence. Naturally, any erosion-induced topography acts to deteriorate the depth resolution attainable in the analysis. A general strategy to minimize crater effects is to restrict the lateral area used for data acquisition

* *Correspondence to: Andreas Wucher, Faculty of Physics, University Duisburg-Essen, 47048 Duisburg, Germany. E-mail: andreas.wucher@uni-due.de*

a *Department of Chemistry, Pennsylvania State University, University Park, PA 16802, USA*

b *Faculty of Physics, University Duisburg-Essen, 47048 Duisburg, Germany*

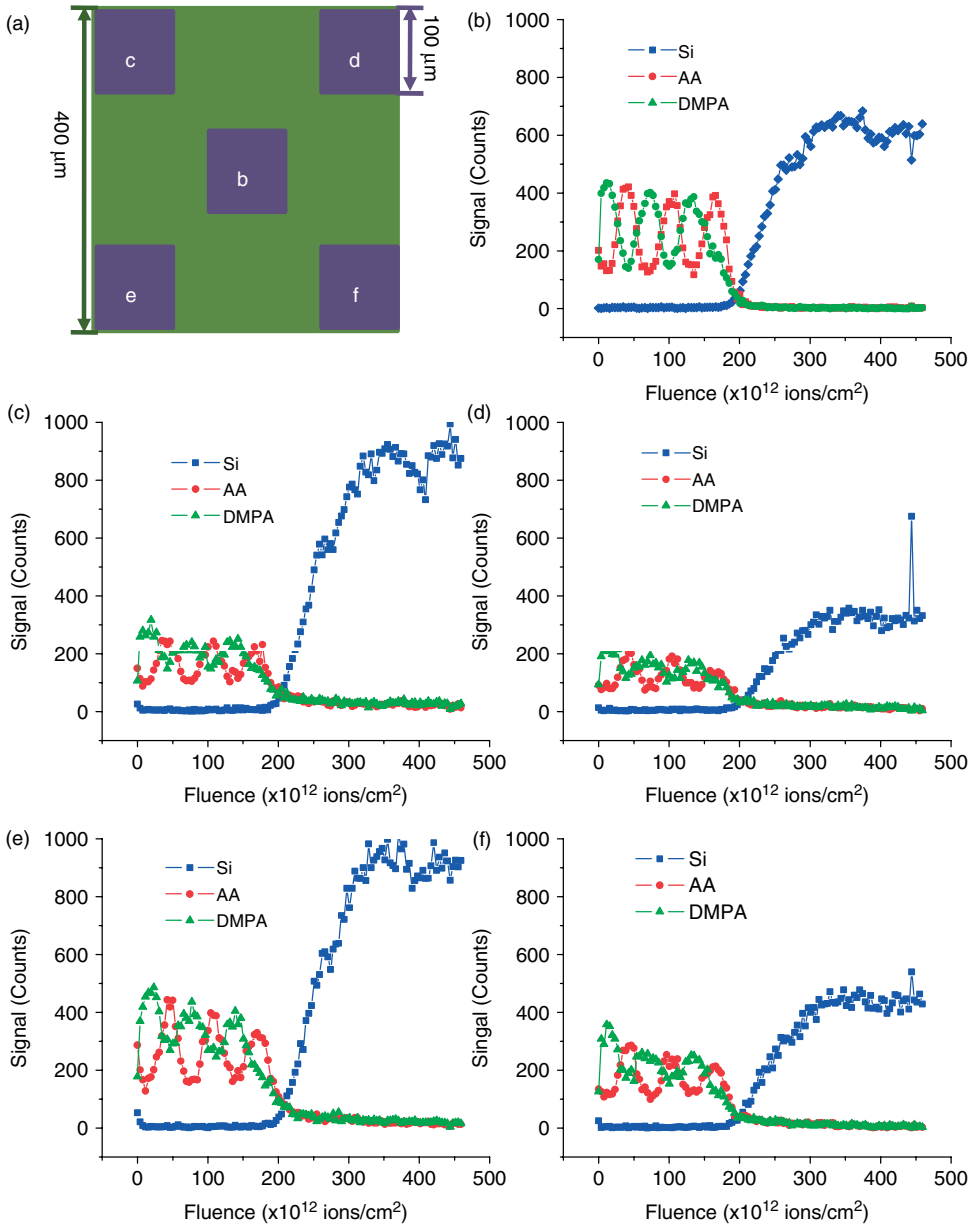

Figure 1. (a) Schematic drawing (ion beam impinging from the bottom) to show the location of gating area used to extract depth profiles displayed in (b)–(f) within the original three-dimensional dataset.

('gating area') as much as possible to the center of the eroded crater. This, however, inevitably leads to a compromise between depth resolution and detection sensitivity, and the gating area must therefore be carefully chosen in order to achieve optimum results. In conventional sputter depth profiling, it is necessary to preselect this area prior to data acquisition, and the only way to judge the suitability of this choice is to acquire multiple depth profiles with different selections. This is where imaging depth profile analysis becomes extremely useful, since it is possible to investigate the influence of the gating area by retrospective analysis of one dataset acquired in one single depth profile measured on the same spot at the sample surface.

In order to investigate how both the size and the position of the gating area within the sputter crater affect the apparent depth resolution, depth profiles extracted from different lateral $100 \times 140\,\mu m^2$ regions of interest within the three-dimensional image stack are compared in Figure 1. It is obvious that the quality of the depth profile greatly depends on the analyzed location within the sputter crater. As expected, the profile taken at the center of the crater (Figure 1(b)) exhibits highest signal contrast for both AA and DMPA, indicating that the optimum depth resolution is achieved under these conditions.

Since the sample is laterally homogenous and the data acquisition is the same in all cases, the reason behind the different performance of these depth profiles must be related to a lateral inhomogeneity of the sputter erosion process. To quantitatively investigate this crater effect further, we examine depth profiles extracted from the center of the crater with different size of the analyzed gating area as shown in Figure 2.

From each of the extracted depth profiles, we calculate an 'interface width' as a measure of the apparent depth resolution using the modulation contrast of the signals as described

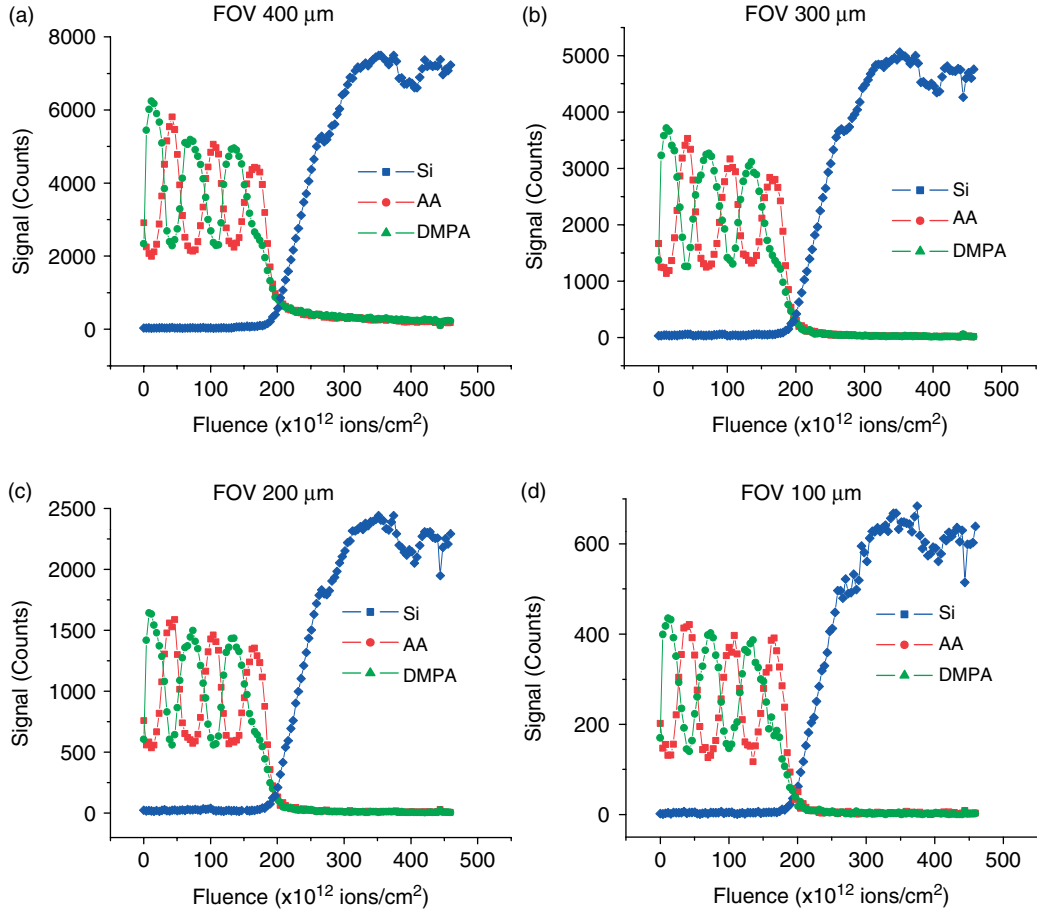

Figure 2. Depth profiles extracted from the 3D image stack using different gating area (FOV) centered within the sputter eroded crater.

earlier.[7] This quantity corresponds to the width (2σ) of an assumed Gaussian-shaped depth response function which would be measured for a delta layer. The resulting values are determined for each interface in the multilayer stack and plotted against the depth of the interface in Figure 3(a). It is seen that in all cases the interface width increases linearly with eroded depth, as would be expected from a lateral inhomogeneity of the erosion rate. Moreover, the apparent width of each individual interface is found to increase with increasing gating area as displayed in Figure 3(b).

In principle, it should be possible to eliminate the effect of *both* a laterally inhomogenous erosion rate *and* bombardment induced dynamics (surface topography generation or mixing) by extrapolating the measured interface width to zero eroded depth. The plot displayed in Figure 3a) shows that these extrapolated 'virtual' interface widths depend on the gating area, indicating that another lateral inhomogeneity besides a crater effect must also influence the apparent depth resolution. Since this cannot be induced by the depth profiling process, it must relate to properties of the original sample itself. The data in Figure 3(b) manifest a linear influence of the gating area which arises from a convolution of lateral inhomogeneities of the sample and the sputter erosion process. As seen from the figure, the influence of such inhomogeneities can be eliminated by extrapolation to zero acquisition area. It is seen that the resulting (virtual) zero area ('spot') interface widths still depend on the depth of the particular interface. This inhomogeneity finding can theoretically be caused by dynamic surface roughening or mixing (shown above) or by large-scale lateral fluctuations of the individual layer thicknesses.

Extrapolating the zero depth values to zero area should completely eliminate the influence of any artifacts arising from lateral inhomogeneity or dynamic surface topography evolution and interface mixing. From Figure 3(b), the resulting virtual interface width is determined as $\Delta z_0 = 13 \pm 1$ nm. AFM measurements of the LB surface topography reveal an rms microroughness of the deposited LB film which is about 10 nm larger than that of the original Si substrate. The lateral wavelength of these fluctuations is of the order of sub-μm and, therefore, not tractable by extrapolation of the acquisition area dependence depicted in Figure 3(b). If these fluctuations would be evenly distributed between the six deposited films, the thickness fluctuation of an individual LB film would be $\Delta d \sim 1.6$ nm, leading to an effective interface broadening of the order of 3 nm or one LB monolayer thickness. We therefore conclude that at least 2–3 nm of the observed interface width may be influenced by such monolayer thickness fluctuations. The remaining interface width of about 10 nm must be attributed to the depth profiling method itself. It is clear that the information depth of static ToF SIMS must contribute to this value. Another contribution arises from the statistics of the sputter removal process, which generates nanometer-scale surface microtopography as soon as the static fluence limit is exceeded. At present, the magnitude of these contributions is not known for organic films. MD simulations performed for inorganic samples bombarded by C_{60} suggest an

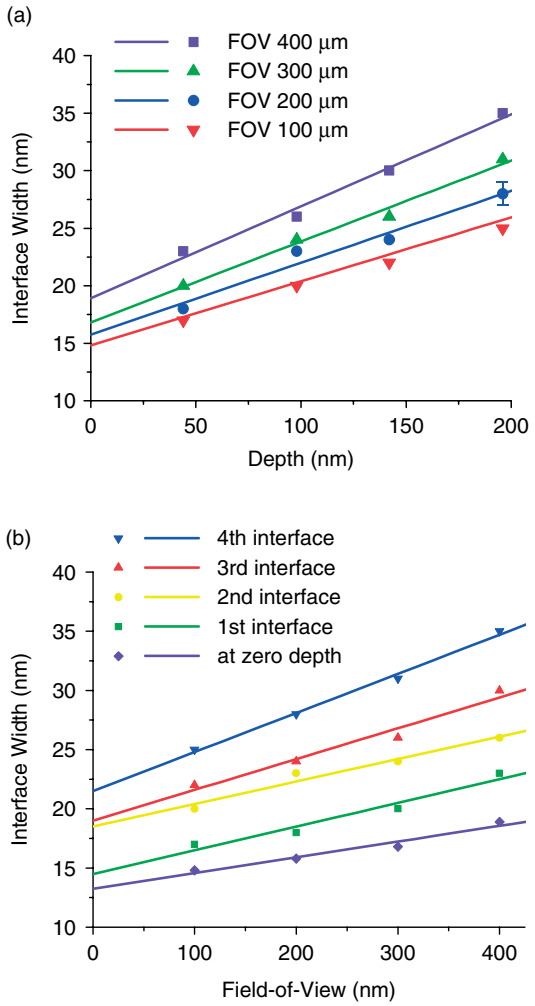

Figure 3. Interface width extracted from depth profiles accumulated over different gating area vs (a) interface depth and (b) size of the gating area.

interface broadening of the order of about 10 monolayers.[10] Keeping in mind that typical molecular monolayer thicknesses are of the order of nanometers (as opposed to Angstroms for inorganic targets), the observed value of Δz_0, therefore, appears reasonable.

Conclusion

The three-dimensional analysis of chemically alternating LB multilayer films provides a suitable platform to investigate different effects contributing to the apparent depth resolution in molecular depth profiling experiments. Comparing depth profiles extracted from different lateral regions of the analyzed area centered around different positions within the sputter crater reveal the role played by lateral inhomogeneities of both the erosion rate ('crater effects') and the sample itself. In this context, the multilayer sample structure is extremely useful, since it allows to investigate the depth-dependent degradation of the apparent depth resolution.

It is found that measured interface widths decrease linearly with decreasing analysis area, thus allowing an extrapolation towards zero analyzed surface area. The 'spot' interface width determined this way is found to increase with increasing eroded depth, again in a linear fashion which allows extrapolation to zero eroded depth. The resulting width of about 13 nm characterizes the apparent depth resolution stripped of broadening effects induced by large-scale lateral inhomogeneities of both the sample and the erosion rate as well as of dynamical evolution of ion bombardment induced surface topography or interface mixing. It does, however, still contain a contribution caused by microscopic fluctuations of the sample film thickness, since these cannot be eliminated by the applied extrapolation procedure. The remaining interface width of the order of 10 nm must be attributed to the depth profiling method itself. This value appears to be in good agreement with data obtained on other molecular systems.[11]

Acknowledgements

Financial support from the National Institutes of Health under Grant # EB002016-16, the National Science Foundation under Grant # CHE-0908226, and the Department of Energy Grant # DE-FG02-06ER15803 are acknowledged.

References

[1] C. M. Mahoney, S. V. Roberson, G. Gillen, *Anal. Chem.* **2004**, *76*, 3199.
[2] A. G. Sostarecz, C. M. McQuaw, A. Wucher, N. Winograd, *Anal. Chem.* **2004**, *76*, 6651.
[3] S. Sun, C. Szakal, T. Roll, P. Mazarov, A. Wucher, N. Winograd, *Surf. Interface Anal.* **2004**, *36*, 1367.
[4] J. Cheng, N. Winograd, *Anal. Chem.* **2005**, *77*, 3651.
[5] J. S. Fletcher, N. P. Lockyer, S. Vaidyanathan, J. C. Vickerman, *Anal. Chem.* **2007**, *79*, 2199.
[6] E. A. Jones, N. P. Lockyer, J. C. Vickerman, *Anal. Chem.* **2008**, *80*, 2125.
[7] L. Zheng, A. Wucher, N. Winograd, *J. Am. Soc. Mass Spectrom.* **2008**, *19*, 96.
[8] L. Zheng, A. Wucher, N. Winograd, *Anal. Chem.* **2008**, *80*, 7363.
[9] R. M. Braun, P. Blenkinsopp, S. J. Mullock, C. Corlett, K. F. Willey, J. C. Vickerman, N. Winograd, *Rapid Commun. Mass Spectrom.* **1998**, *12*, 1246.
[10] K. D. Krantzman, A. Wucher, *J. Phys. Chem.* **2010**, *114*, 5480.
[11] A. Wucher, J. Cheng, L. Zheng, D. Willingham, N. Winograd, *Appl. Surf. Sci.* **2008**, *255*, 984.

